MEASUREMENT OF INTERNAL AND SURFACE TEMPERATURES AND OPTICAL PROPERTIES OF ZERDINE PHANTOM UNDER 635 NM LOW LEVEL LASER IRRADIATION

HÜSEYIN OKAN DURMUŞ[1,2], MIRHASAN Yu. SEYIDOV[1]
[1]Department of Physics, Gebze Technical University, 41400, Kocaeli, Turkey
[2]Medical Metrology Laboratory, TUBITAK National Metrology Institute (TUBITAK UME), 41470, Kocaeli, Turkey
E-mail: hokandurmus@gtu.edu.tr, smirhasan@gtu.edu.tr;
Tel: (262) 605 10 00; Fax: (262) 653 84 90

In this study, internal and surface temperatures of the Zerdine phantom used as reference material in the ultrasonic imaging processes and its optical properties such as absorbance, transmittance, reflectance, refractive index, and optical attenuation coefficient were investigated by using a low-level laser device which has a 635 nm wavelength. Internal temperatures and the said optical properties were measured successfully. However, due to the transparent color nature of the Zerdine phantom, significant temperature increases could not be detected at the surface of the phantom. Therefore, the phantom material was colored at different concentrations with a color tone close to human skin, and thus surface temperatures were measured in this way. However, it was determined that surface temperature values did not increase too much with increasing color concentration. Therefore, it has been concluded that the use of Zerdine phantom as an ideal background reference material in optical imaging studies makes it advantageous because of its transparent color nature and low optical absorbance value.

Keywords Low-Level Laser, Zerdine Phantom, Internal and Surface Temperature Measurements, Optical Properties.

INTRODUCTION

Today, lasers are used extensively in all areas of life. However, medical lasers are one of the most effective, intensive and widely used devices. The use of lasers in diagnostic and therapeutic applications varies according to the place of use. Therefore, laser researchers have developed different lasers for different medical needs in medical operations and treatments. Dermatology, ophthalmology, dentistry, otolaryngology, gastroenterology, urology, gynaecology, cardiology, neurosurgery and orthopaedics can be given the examples of areas where lasers are used. In addition, there is also every day of new developments in laser-based techniques. In particular, the role of light-based technologies in dermatology has increased dramatically in recent years. Therefore, laser or light-based therapy devices for the treatment of dermatological diseases are constantly being introduced [1-6].

The use of low-level lasers has gained popularity in the medical sciences over the last 30 years [7]. Low Level Laser Therapy (LLLT, or sometimes also called as Low Level Light Therapy or Photobiomodulation (PBM)) is a low intensity light therapy. Usually low power laser (typically in the power range of 10 mW-500 mW) or LED light is applied to the skin in this therapy. For a long time, low-level laser therapy (LLLT) or LED (light emitting diode) photobiomodulation has been shown to reduce inflammation and edema, induce analgesia (relieve pain), and promote healing musculoskeletal pathologies and injured tissues [8-9]. In clinical practice, the effect of temperature on tissue is the most common category of laser-tissue interaction, as well as photo-chemical and photo-mechanical effect [10].

Tissue-mimicking materials (TMMs) or tissue phantoms are widely used in the biomedical research area especially at thermo-acoustical [11-14] and optical research [15-18] as a test model.

The definition of the phantom is made as “any apparatus or material that mimics the operation or physical properties of human systems or tissues”. Although it is possible to use real tissues directly in experiments, this is not a logical method. Instead, working with artificial materials that simulate the physical properties (such as acoustical, optical, mechanical and thermal, etc.) of human tissues provides many benefits. Therefore, phantoms enable systematic testing and controlled optimization of new measurement methodologies before being tested on living things such as animals or humans. The use of phantoms enables simulation for systems at different complexity levels or human tissues. The use of phantoms in initial tests instead of biological materials provides an effective alternative to medical research. Therefore, after the initial results on phantoms are positive, real tissues can be used. After this stage, animal experiments (laboratory mice in general) are usually performed, and then the tests are performed on humans [19].

In the optical field, phantoms are used in various forms such as the development of imaging techniques and image-guided interventions, system validation, optimization, stability assessment, medical device calibration, verification, and clinical training [20-22].

In this study, internal and surface temperatures caused by 635 nm low level red color laser irradiation on Zerdine phantom were measured and optical properties of the phantom were determined. With this study carried out, the temperature effects of a low level laser device on a tissue-phantom and thus the safety usage of the laser will be investigated. Therefore, this investigation will provide an innovative contribution to the scientific literature in terms of safety evaluation.

131, H.Javid ave, AZ-1143, Baku
ANAS, Institute of Physics
E-mail: jophphysics@gmail.com

The organization of the paper will be as follows. In the second part, information about phantom material, the laser used, thermal camera and surface temperature measurements, optical power meter, thermal sensor and optical power measurements, single integrating sphere and measurement and calculation of optical properties will be given. In the third part, internal temperature measurements, surface temperature measurements, and optical power measurements results will be shared. In the final section, the studies made and the results obtained will be summarized and some suggestions will be given.

METHODOLOGY

In this study, the colored and transparent Zerdine phantom, laser device, T-type of thermocouples, single integrating sphere, optical power meter and its thermal sensor and infrared/thermal camera were used. All experiments were performed under controlled laboratory ambient conditions.

PREPARATION OF ZERDINE PHANTOM

The Zerdine phantom was produced according to the formula of Zerhouni and Rachedine. The colored phantom samples were prepared from the stock solution prepared with brown, yellow and pink water-based dyes in the amount of 0.375 ml (2.5%), 0.75 ml (5%), 1.5 ml (10%), 3 ml (%20) by putting together with Zerdine phantom within 15 ml containers. A picture of different colored Zerdine phantoms can be seen in Figure 1.

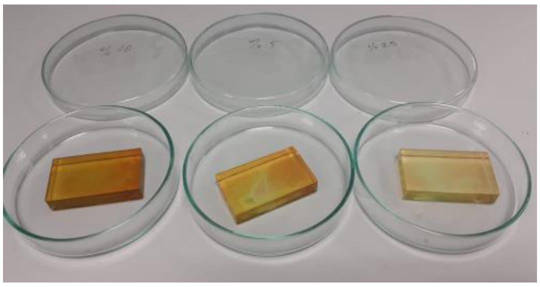

Fig. 1. A picture of the colored Zerdine phantoms.

THE LASER USED

Optotronics brand VA-I-400-635 model 635 nm wavelength red color solid-state diode laser was used for the measurements as an optical source. Maximum working power of the laser was 400 mW.

TERMOCOUPLE POSITION WITHIN PHANTOM AND INTERNAL TEMPERATURE MEASUREMENT

For internal temperature measurements, Physitemp T-type ultra-fine termocouples were loacted at 15 mm inside from the phantom surface. The distance between the thermocouples was designed to be as 2 mm apart. For multi-channel temperature measurements within the phantom, a PC-based Data Acquisition and Monitoring Interface system was used. Internal temperature measurement set-up can be seen in Figure 2.

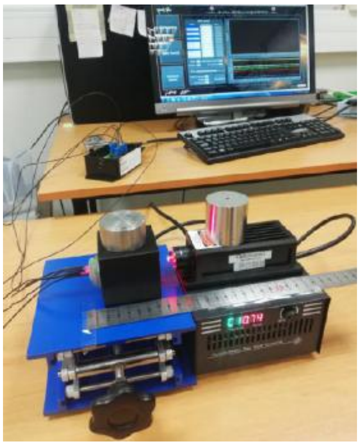

Fig. 2. Internal temperature measurement set-up.

THERMAL CAMERA AND SURFACE TEMPERATURE MEASUREMENT

Optris PI infrared/thermal camera as shown in Figure 3 and its PC software were used for surface temperature measurements. The declared uncertainty budget for the infrared camera was ± 2 °C as stated in the product catalog.

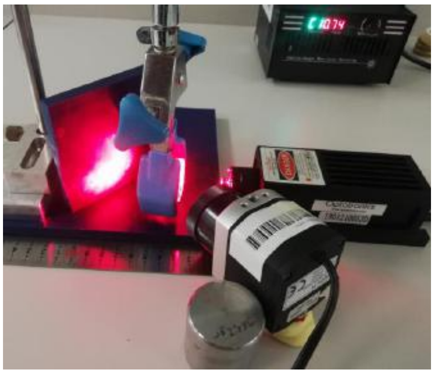

Fig. 3. A picture of pure Zerdine phantom temperature measurement set-up with infrared/thermal camera.

A picture of temperature measurement set-up with infrared/thermal camera for the deliberately colored Zerdine phantom can be seen in Figure 4.

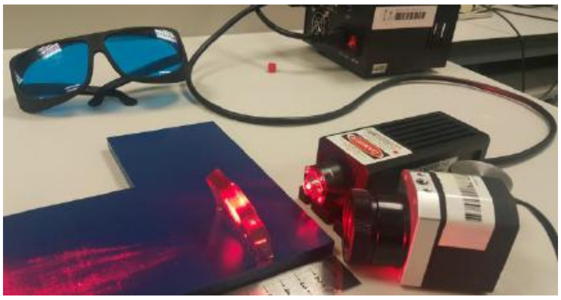

Fig. 4. A picture of temperature measurement set-up with infrared/thermal camera for the deliberately colored Zerdine phantom.

OPTICAL POWER METER, THERMAL SENSOR AND OPTICAL POWER MEASUREMENT

Ophir brand StarBright model optical power meter and Ophir brand 3A type thermal sensor were used for optical power measurements. Figure 5 shows optical power meter, thermal sensor and picture of optical power measurements. Optical Power Measurement set-up can be seen in the Figure 5.

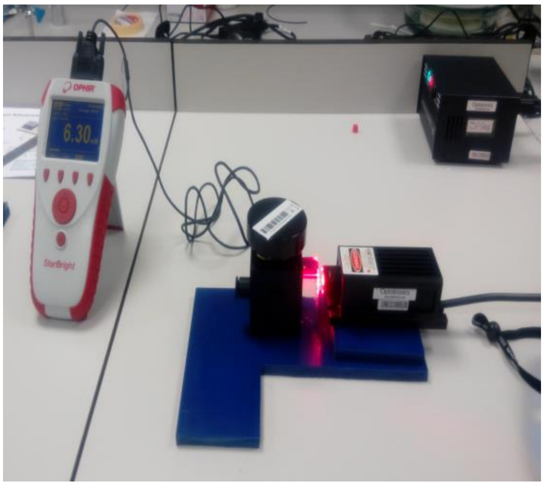

Fig. 5. Optical Power Measurement Set-up.

SINGLE INTEGRATING SPHERE AND MEASUREMENTS OF OPTICAL PROPERTIES

Thorlabs IS200 model 2” integrating sphere was used in the measurement of optical properties such as absorbance, transmittance, reflectance, refractive index and optical attenuation coefficient.

CALCULATION OF OPTICAL PROPERTIES

Optical properties such as absorbance, transmittance, reflectance, the refractive index, and optical attenuation coefficient were calculated by using the following formulas.

$$R+T+A = 1 \text{ or } \%R+\%T+\%A = \%100 \qquad [23]\ (1)$$

Absorbance,

$$A;\ A=-\log(I/I0)=-\log(T)=2-\log(\%T) \qquad [24]\ (2)$$

$$\text{Transmittance, } T;\ T = I/I0 \qquad [24]\ (3)$$

$$\text{Reflectance, } R;\ R=1-(A+T) \qquad [23]\ (4)$$

$$\text{Reflectance, } R = \frac{(n-1)^2}{(n+1)^2}, \qquad [23]\ (5)$$

where n is the Refractive Index.

$$I = I_0 e^{-\mu x},\ \mu = -\frac{\ln\frac{I}{I_0}}{x} \qquad [25]\ (6)$$

Where μ is the Linear Attenuation Coefficient.

RESULTS AND DISCUSSION

INTERNAL TEMPERATURE MEASUREMENTS

Internal temperature measurements were carried out for 60 seconds duration at each step by increasing the laser distance by 5 mm from the phantom surface between 5 mm and 25 mm. The internal temperatures measured can be seen below from Figures 6 up to 10.

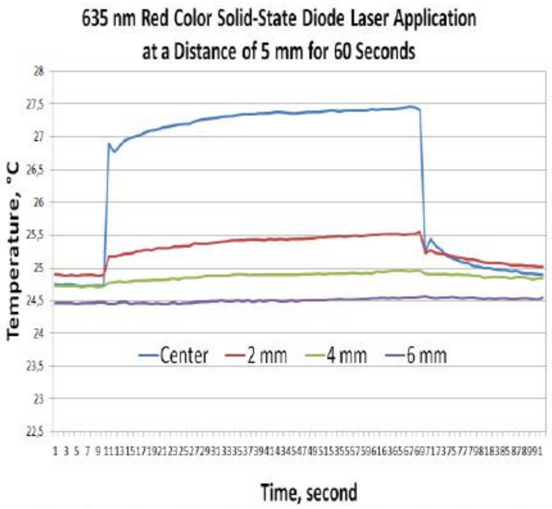

Fig. 6. The internal temperature measurements at a distance of 5 mm for laser irradiation applied for one minute.

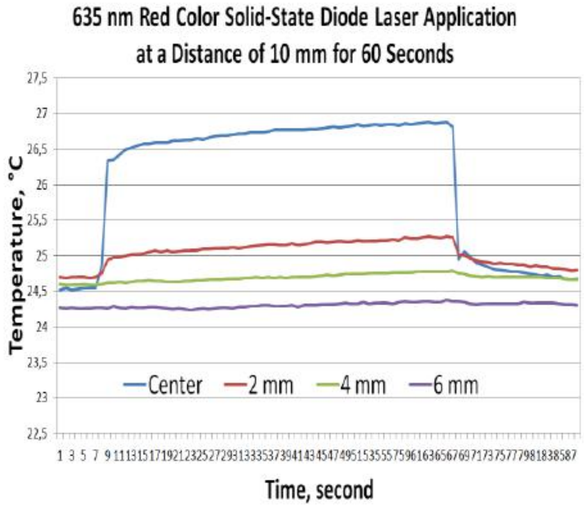

Fig. 7. The internal temperature measurements at a distance of 10 mm for laser irradiation applied for one minute.

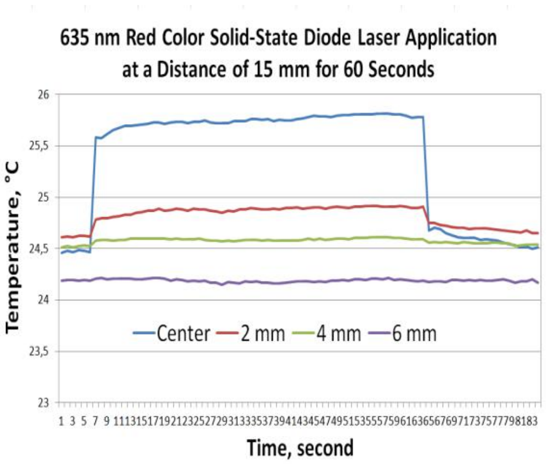

Fig. 8. The internal temperature measurements at a distance of 15 mm for laser irradiation applied for one minute.

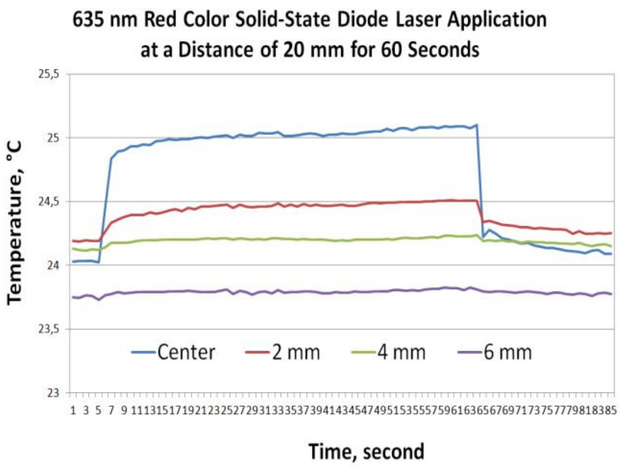

Fig. 9. The internal temperature measurements at a distance of 20 mm for laser irradiation applied for one minute.

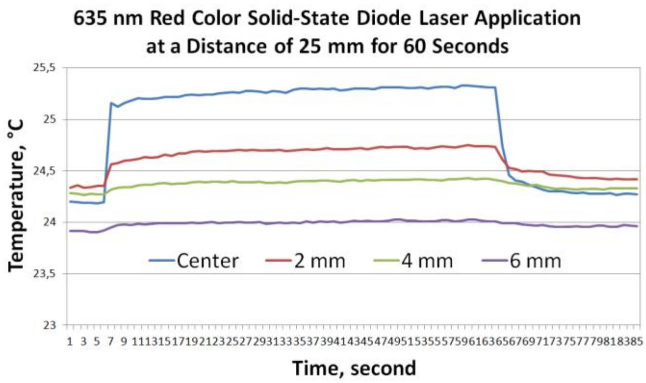

Fig. 10. The internal temperature measurements at a distance of 25 mm for laser irradiation applied for one minute.

The minimum and maximum temperatures, and temperature differences measured at different thermocouple locations within the phantom can be seen from Figure 11 to Figure 15.

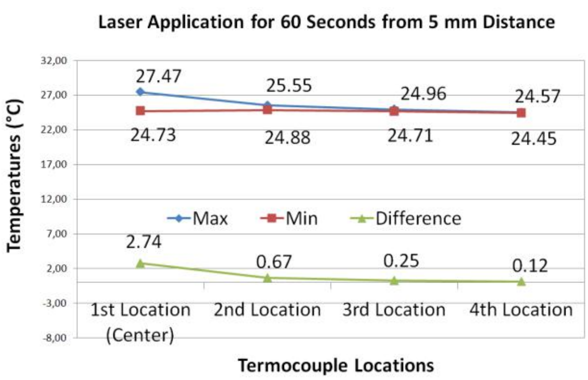

Fig. 11. Maximum and minimum temperatures, and temperature differences at different thermocouple locations caused by a distance of 5 mm.

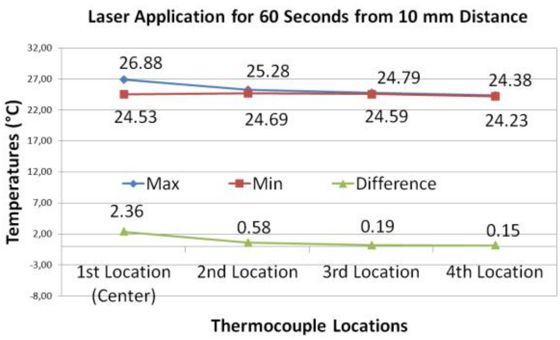

Fig. 12. Maximum and minimum temperatures, and temperature differences at different thermocouple locations caused by a distance of 10 mm

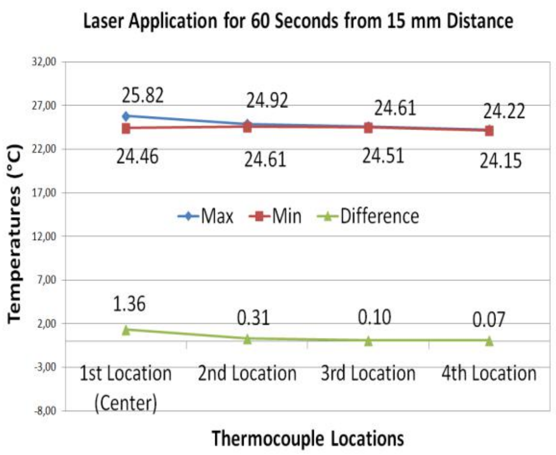

Fig. 13 .Maximum and minimum temperatures, and temperature differences at different thermocouple locations caused by a distance of 15 mm.

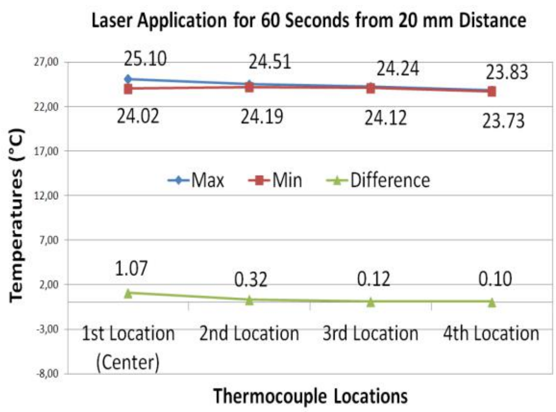

Fig. 14. Maximum and minimum temperatures, and temperature differences at different thermocouple locations caused by a distance of 20 mm.

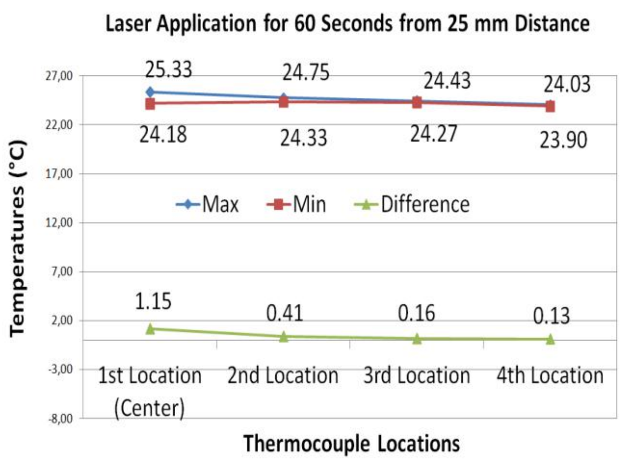

Fig. 15. Maximum and minimum temperatures, and temperature differences at different thermocouple locations caused by a distance of 25 mm.

By using above results, we can reorganize and evaluate the temperature differences in a good manner as per thermocouples used within the phantom. The temperature differences measured by the thermocouples according to the distance of the laser beam from the phantom surface can be seen from Figure 16 to Figure 19.

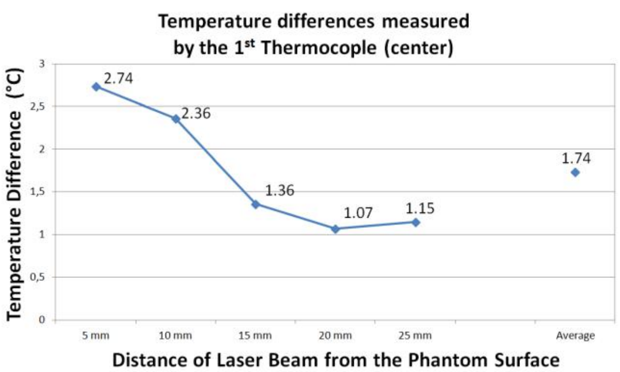

Fig. 16. The temperature differences measured by the 1st thermocouple (center thermocouple) within the phantom

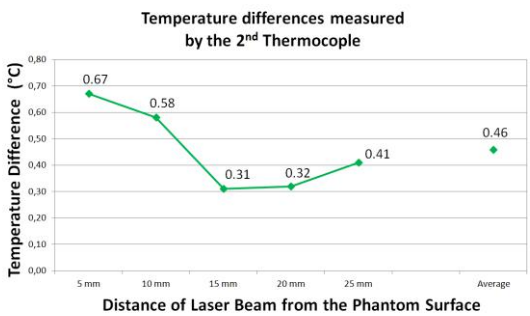

Fig. 17. The temperature differences measured by the 2nd thermocouple within the phantom

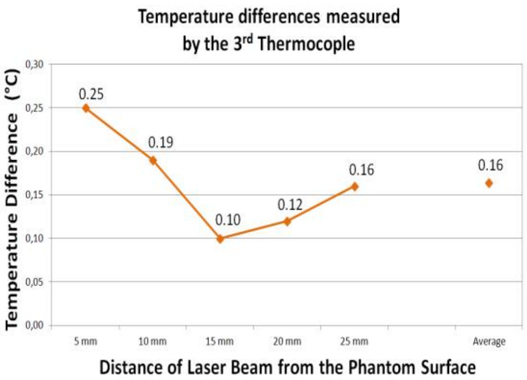

Fig. 18. The temperature differences measured by the 3rd thermocouple within the phantom.

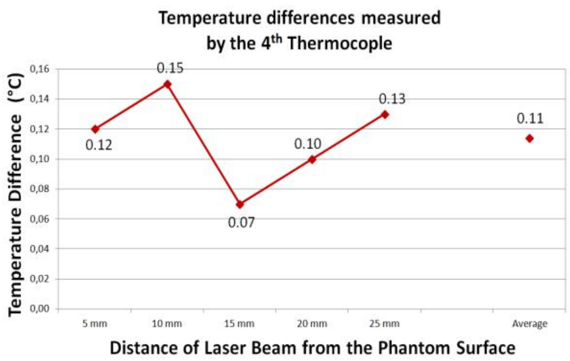

Fig. 19. The temperature differences measured by the 4th thermocouple within the phantom.

SURFACE TEMPERATURE MEASUREMENTS

Because of the transparent color of the Zerdine phantom, significant temperature rises at surface temperatures could not be detected. Thus, the phantom material was colored at different concentrations as 2.5%, 5%, 10% and 20% with a color tone close to human skin (near to red skin) and the temperature differences formed at the phantom surface were measured within one minute interval at different distances with the laser “on” and “off” position. The measurement results can be seen from Figure 20 up to Figure 24.

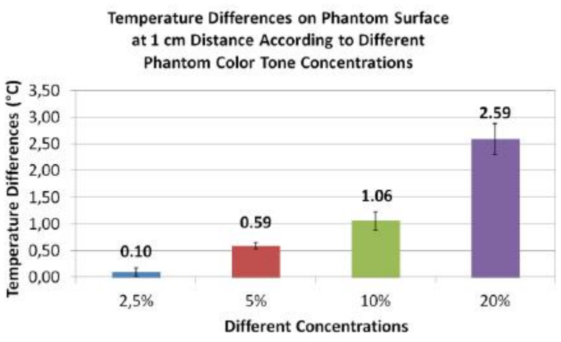

Fig. 20. The measured average temperature differences on phantom surface at 1 cm distance as per different color tone concentartions

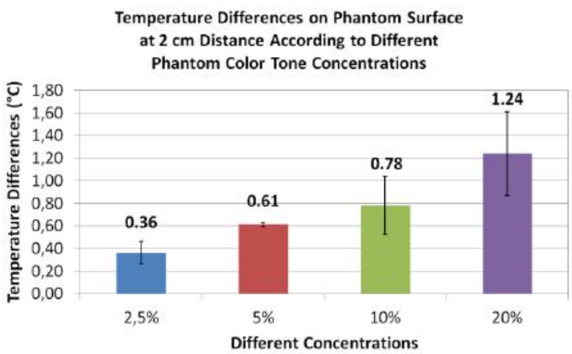

Fig. 21. The measured average temperature differences on phantom surface at 2 cm distance as per different color tone concentartions

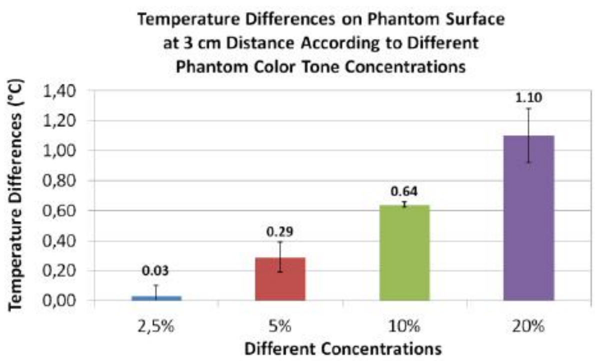

Fig. 22. The measured average temperature differences on phantom surface at 3 cm distance as per different color tone concentartions.

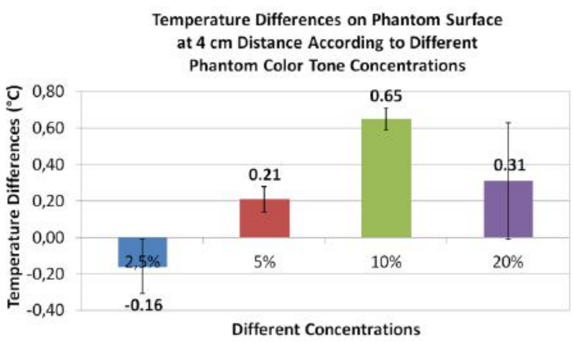

Fig. 23. The measured average temperature differences on phantom surface at 4 cm distance as per different color tone concentartions.

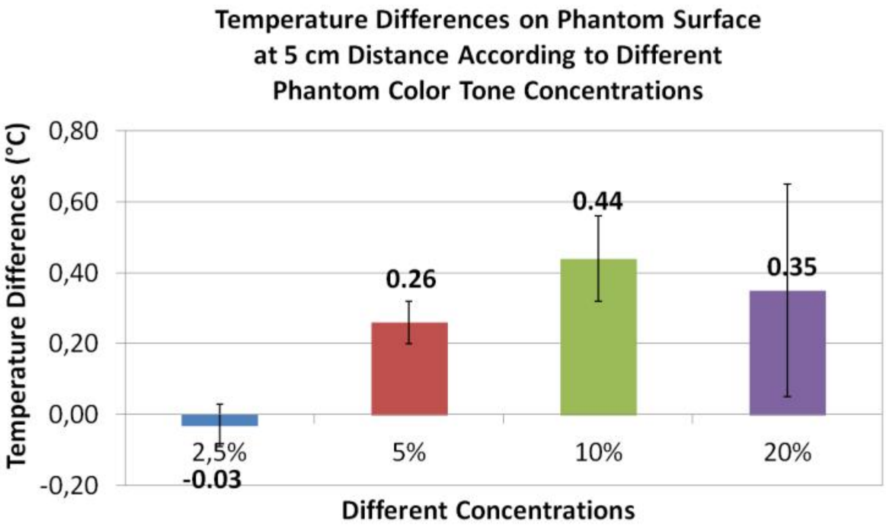

Fig. 24. The measured average temperature differences on phantom surface at 5 cm distance as per different color tone concentartions.

MEASUREMENTS OF OPTICAL PROPERTIES

The measurement of optical properties at 635 nm was performed using the single integrating sphere set-up. The measured values of optical properties of the Zerdine phantom at 635 nm can be seen in Figure 25 and Table I. As seen from the figure that transmittance value of the Zerdine phantom is high. This means that Zerdine phantom behaves like a glass. Because most of the light rays pass through of it.

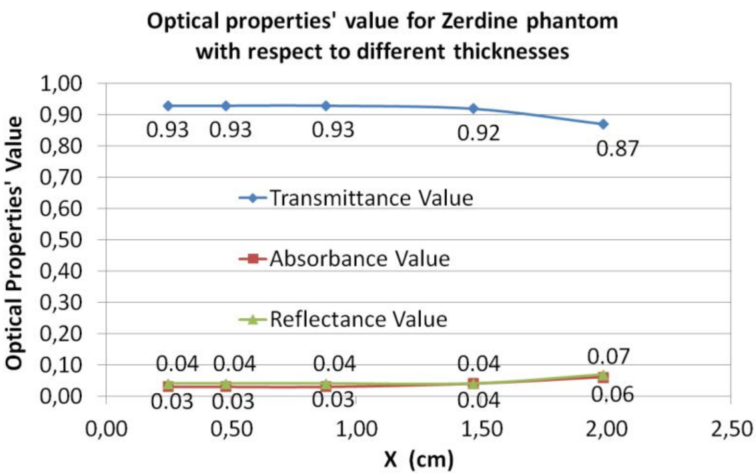

Fig. 25. The measured values of optical properties of the Zerdine phantom.

Table I.

The measured optical properties of the Zerdine phantom at 635 nm as average

Phantom	Transmittance, T	Absorbance, A	Reflectance, R	Attenuation Coefficient (cm^{-1})
Zerdine	0,91 ± 0.03	0,04 ± 0.01	0,05 ± 0.01	0,028 ± 0.01

The attenuation coefficient for Zerdine phantom at 635 nm was found as 0,028 cm^{-1} as can be seen in Table I and Figure 26.

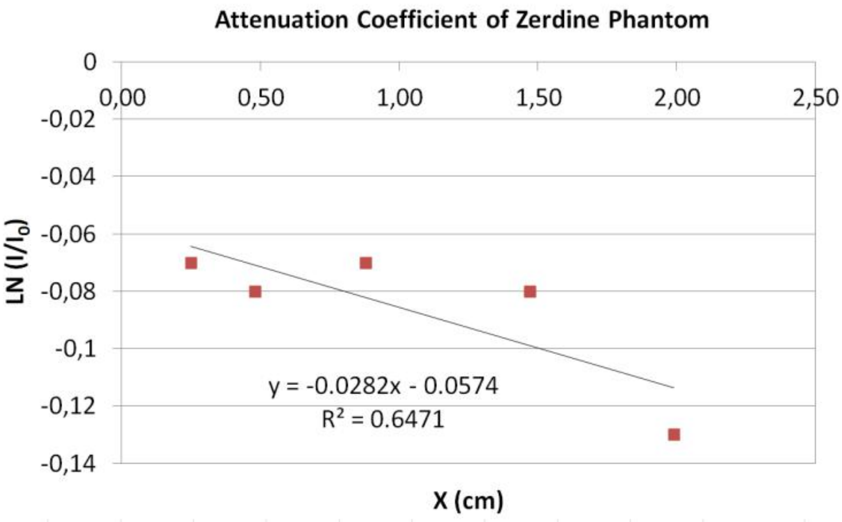

Fig. 26. The attenuation coefficient drawing graph for Zerdine phantom.

Using the formula (5), we also calculated the refractive index at 635 nm and we found the refractive index as 1.58 ± 0.08. This value also explains and proves the glass-like nature of the Zerdine phantom. Because the range of refractive indecies of the glass has a value between 1.4 and 1.7 [26].

CONCLUSION

In this study, it was firstly tried to be investigated the internal temperature values on Zerdine phantom under 635 nm low level laser irradiation. Later, surface temeperatures of deliberately colored Zerdine phantom were measured. Finally, the optical properties of colorless Zerdine phantom were determined.

As a result, this research study can be summarized as follows.

- This study has shown that low-level laser irradiation can be used together with phantom studies. Therefore, phantom studies can be used for optical and temperature characterization of low level lasers.
- Low level laser irradiation produced insignificant temperature increases (max. about 3 °C) within the phantom and phantom surface.
- Low level laser irradiation was found as a safe application on human use for 1 minute interval at a distance of min 0.5 cm in our investigation. Other studies should also be carried out with long periods.
- The Zerdine phantom's optical properties such as absorbance, transmittance, reflectance, the refractive index, and optical attenuation coefficient at 635 nm were investigated for the first time in our knowledge.
- These studies may be evaluated as a tool in the development of wavelength sensitive optical phantom in the future.
- It is also very logical and advantageous to use the Zerdine phantom in terms of optical properties as an ideal background reference material in optical imaging studies because of its transparent color nature and low optical absorbance value.

As a result of this study, we can say that low-level laser therapy sources can be examined by using phantom studies. Furthermore, this study can also be extended towards different kinds of phantoms, the optical properties of the phantoms can be determined in this way and much more similar research studies can be done in the future.

[1] *M.A. Ansari ve E. Mohajerani*. «Mechanisms of Laser-Tissue Interaction: I. Optical Properties of Tissue,» Journal of Lasers in Medical Sciences, cilt 2, no. 3, pp. 119-125, Summer 2011.

[2] *Q. Peng, A. Juzeniene, J. Chen, L.O. Svaasand, T. Warloe, K.E. Giercksky, J. Moan.* 2008. Lasers in medicine. Reports on Progress in Physics, 71(5), 056701.

[3] *L.O. Svaasand.* «Laser-tissue interaction,» Proc. SPIE 1524, Bioptics: Optics in Biomedicine and Environmental Sciences, pp. 1-13, 1992.

[4] *B. Dinç ve M.E. Or.* «Farklı Tipte Lazerlerin Veteriner Hekimlikte Kullanımı,» TÜBAV Bilim, cilt 7, no. 3, pp. 1-10, 2014.

[5] *Z. Husain ve T. S. Alster.* «The role of lasers and intense pulsed light technology in dermatology,» Clinical, Cosmetic and Investigational Dermatology, no. 9, pp. 29-40, 2016.

[6] *K.J. Ahn, B.J. Kim ve S.B. Cho.* «Tissue-Mimicking Phantom Useful in Simulating Laser Light Tissue Interactions» Medical Lasers, cilt 4, no. 2, pp. 86-88, 2015.

[7] *Y. Alipanah, M. Asnaashari ve F. Anbari.* «The effect of low level laser (GaAlAs) therapy on the post-surgical healing of full thickness wounds in rabbits,» Medical Laser Application, no. 26, pp. 133-138, 2011.

[8] *H.B. Cotler, R.T. Chow, M.R. Hamblin, J. Carroll.* 2015. The use of low level laser therapy (LLLT) for musculoskeletal pain. MOJ orthopedics & rheumatology, 2(5).

[9] *G.K. Reddy, L. Stehno-Bittel, C.S.Enwemeka.* 1998. Laser photostimulation of collagen production in healing rabbit Achilles tendons. Lasers in Surgery and Medicine: The Official Journal of the American Society for Laser Medicine and Surgery, 22(5), 281-287.

[10] *A.L. McKenzie.* «Physics of thermal processes in laser-tissue interaction,» Phys. Med. Biol., cilt 35, no. 9, pp. 1175-1209, 1990.

[11] *B. Karaböce.* 2015, May. Focused ultrasound temperature effect in tissue-mimicking material and sheep liver. In 2015 IEEE International Symposium on Medical Measurements and Applications (MeMeA) Proceedings (pp. 131-134). IEEE.

[12] *B. Karaböce, H.O. Durmuş.* 2015. Visual investigation of heating effect in liver and lung induced by a HIFU transducer. Physics Procedia, 70, 1225-1228.

[13] *B. Karaböce, E. Çetin, H.O. Durmuş*. 2016, May. Investigation of temperature rise in tissue—Mimicking material induced by a HIFU transducer. In 2016 IEEE International Symposium on Medical Measurements and Applications (MeMeA) (pp. 1-6). IEEE.

[14] *B. Karaböce, E.Çetin, H.O. Durmuş, M. Özdingiş, H. Öztürk, K. Mahmat, M. A. Güler.* 2018, June. Investigation of Different TMMs in High Intensity Focused Ultrasound Applications. In 2018 IEEE International Symposium on Medical Measurements and Applications (MeMeA) (pp. 1-5). IEEE.

[15] *B.W. Pogue, M.S. Patterson.* 2006. Review of tissue simulating phantoms for optical spectroscopy, imaging and dosimetry. Journal of biomedical optics, 11(4), 041102.

[16] *İ. Akkaya, M. Engin, Y. Öztürk.* Doku Fantom Üretimi ve Temel Optik Özelliklerinin Ölçümü/Fabrication of Tissue Phantom and Measurement of The Fundamental Optical Properties. Celal Bayar Üniversitesi Fen Bilimleri Dergisi, 13(1), 2017, 205-209.

[17] *J. ZHANG, L.I.U. Yuanjie, J.ROBIC, A. NKENGNE, Y.A.N. Hong, X. ZHANG, SOO, X.Y.* 2019. Optical Phantom Development for Skin Measurement. In 19th International Congress of Metrology (CIM2019) (p. 19001). EDP Sciences.

[18] *R. Srinivasan, D. Kumar, M. Singh*. 2002. Optical tissue-equivalent phantoms for medical imaging. Trends Biomater. Artif. Organs, 15(2), 42-47.

[19] *R.A. Jaime, , Basto, R. L., Lamien, B., Orlande, H. R., Eibner, S., & O. Fudym,* (2013). Fabrication methods of phantoms simulating optical and thermal properties. Procedia Engineering, 59, 30-36.

[20] *A.I. Chen, M.L. Balter, M.I. Chen, D. Gross, S.K. Alam, T.J. Maguire, M.L. Yarmush.* 2016. Multilayered tissue mimicking skin and vessel phantoms with tunable mechanical, optical, and acoustic properties. Medical Physics, 43 (6), 3117-3131.

[21] *P. Lai, X. Xu, L.V. Wang.* 2014. Dependence of optical scattering from Intralipid in gelatin-gel based tissue-mimicking phantoms on mixing temperature and time. Journal of biomedical optics, 19(3), 035002.

[22] *E. Dong, Z. Zhao, M. Wang, Y. Xie, S. Li, P. Shao, R.X. Xu.* 2015. Three-dimensional fuse deposition modeling of tissue-simulating phantom for biomedical optical imaging. Journal of biomedical optics, 20(12), 121311.

[23] *M.Y. Nadeem, W. Ahmed.* 2000. Optical properties of ZnS thin films. Turkish Journal of Physics, 24(5), 651-659.

[24] *D.T. Harvey.* 2003. Analytical Chemistry for Technicians, 3rd Edittion, page 193, (John Kenkel).

[25] *S. Chang, A.K. Bowden.* 2019. Review of methods and applications of attenuation coefficient measurements with optical coherence tomography. Journal of biomedical optics, 24(9), 090901.

[26] *J. Fraser, R. Williams.* 2009. Page 192, Handbook of Forensic Science.

Received: 05.09.2022